Analyst

Accepted Manuscript

ROYAL SOCIETY OF CHEMISTRY

www.rsc.org/analyst

Time-resolved ICP-MS Analysis of Mineral Element Contents and Distribution Patterns in Single Cells

Hailong Wang,[#] Bing Wang,[#] Meng Wang, Lingna Zheng, Hanqing Chen, Zhifang Chai, Yuliang Zhao, Weiyue Feng*

CAS Key Laboratory for Biomedical Effects of Nanomaterials and Nanosafety, CAS Key Laboratory of Nuclear Radiation and Nuclear Energy Technology, Institute of High Energy Physics, Chinese Academy of Sciences, Beijing 100049, China

[#] These authors contributed equally to this work

[*] Corresponding Author: E-mail: fengwy@ihep.ac.cn

Abstract

Novel single cell techniques are attracting increasing interest for the clinical application because they can elucidate the cellular diversity and heterogeneity instead of the average masked by bulk measurements. Herein, the time-resolved ICP-MS for the determination of essential mineral elements in single cells has been developed and is used to analyze the contents and distribution patterns of Fe, Cu, Zn, Mn, P and S in two types of cancer cells (Hela and A549) and one type of normal cells (16HBE). The results show that there are obvious differences in contents and distribution patterns of the elements among the three types of cells. The mass of Fe, Zn, Cu, Mn, P, and S in individual Hela cells is significantly higher and span a broader range of values than in single 16HBE and A549 cells. The contents of Fe, Zn, and Cu follow log-normal distributions, and Mn, P, and S follow Poisson distributions with high λ values in single Hela cells, indicating a large cell-to-cell variance. Comparatively, the contents of Cu, Zn, P, and S in 16HBE cells show the narrowest distribution-range among the three tested cells, presenting the homogenous distribution of the elements in the cells. The method of single cell ICP-MS (SC-ICP-MS) provides potential application for the monitoring of the variation of mineral elements at a single cell level.

Keywords: Time-resolved ICP-MS; single cell analysis; mineral element distribution; cells.

Introduction

Recent genome-wide assays have revealed that cellular heterogeneity is a widespread event within an isogenic cell population, which is associated with different cell type, physiological feature, bio-environment, and therapeutic response.[1, 2] Thus, single cell analysis (SCA) can provide the valuable information of cell-to-cell variance and identify the rare cell type in a mixed population of cells, which are important for the need of cancer research as well as the basic biomedical study and the fundamental principle of cell biology.[3] So far, multiple novel single-cell techniques, such as genomics, transcriptomics, proteomics, and metabolomics at a single cell level that directly analyze the changes from the chemical contents (genes, proteins and metabolites) of individual cells, have emerged, which exhibit potential applications in the identification and detection of circulating tumor cells,[2] embryo development at early stage,[4] and monitoring immune responses.[5] However, single cell analysis is still in its infancy. There is a great demand to develop new techniques for achieving high temporal, spatial and molecular resolution at a single cell level that can differ significantly from the average patterns over the cell populations.

The endogenous trace metals (*e.g.*, Fe, Cu, Zn, Mn and Co) and non-metals (*e.g.*, P and S) are essential and important constituents in cells, which are found in metalloproteins, metalloenzymes, nuclei acid, adenosine triphosphate (ATP), etc., and play critical roles in a myriad of biological processes, such as oxidative-reductive balance, gene expression, cell cycle regulation and energy metabolism.[6-8] The contents of these essential elements in biological tissue or cells are associated with various patho-physiological conditions.[9] For instance, the cellular requirement for Fe is directly correlated with the cell type, the rate of cell growth, and the stage of cell differentiation. Neoplastic cells are found to have higher iron requirements than normal, non-malignant cells. Fe levels have been found elevated in serum and tumor tissues of many types of cancer patients, including breast cancer, leukaemia, cervical carcinoma, bladder cancer, lung cancer and so forth.[10,11] In addition, the elevated iron levels have

been shown to correlate with tumor angiogenesis, tumor growth and progression.[10,12] Intracellular iron depletion leads to G1/S cell-cycle arrest, DNA damage, and apoptosis.[13] Likewise, a number of tissue abnormalities and disease states in humans have been reported to associate with either reduced or elevated levels of copper.[14] Serum and tumor copper levels are elevated in both solid tumor and blood cancer, and have been reported to directly associate with the severity and progression of cancer, involving in modulating tumor angiogenesis and affecting oxidative stress and so forth in cancer cells.[15] However, the knowledge about to what extent does the metal content heterogeneity and how much diversity of them between normal cells and cancer cells is still limited to date. To explore these questions, we developed a SCA technique based on inductively coupled plasma mass spectrometry (ICP-MS) to determine endogenous elements (Fe, Cu, Zn, P and S) at a single cell level from several batches of human cancer cells and normal cells.

ICP-MS is one of the most useful methods for ultratrace element analysis due to its extremely high sensitivity to a wide range of elements. Recently, time-resolved ICP-MS (usually using a quadrupole analyzer) and ICP-MS applied mass cytometry (usually using a time of flight analyzer) is receiving much attention for elemental and multiparametric analysis of single cells.[16,17] As for single cell ICP-MS (SC-ICP-MS) analysis, the intensity of spike signal is proportional to the quantity of the analyte ions in a cell and the distribution of spike intensity is correlated with the mass distribution of analyte ions in cells.[18] So far, SC-ICP-MS has been used to determine the intracellular major elements such as calcium[19] and magnesium,[9] or exogenous uranium,[20] bismuth-based drugs,[21] and quantum dots[18] in single cells. Through combination with elemental tagged techniques, intracellular biomolecules, including surface antigens, amino acids, peptides, proteins, and DNA, can be successfully quantified in single cells by mass cytometry.[17] In recent years, although the application of time-resolved ICP-MS in SCA has made great progress in single cell analysis,[22,23] the accurate determination of essential mineral elements, *e.g.* Fe, Cu, Zn, Mn, P, and S in mammalian cells, because of the insufficient detection limits, overlapping of spike signals and high cellular background.

In the study, the contents and distribution patterns of essential mineral elements Fe, Cu, Zn, Mn, P, and S in human cancer cells, including human cervical carcinoma (Hela), human lung carcinoma epithelial cell line (A549), and human bronchial epithelial cells (16HBE) at single cell level were analyzed by time-resolved ICP-MS,

which will provide the multiparametric analysis of cellular heterogeneity and may help to understand the behavior of mineral elements in tumor cells and further distinguish the tumor cells from the normal ones. The unique analytical capability of SC-ICP-MS for the essential mineral elements in single cells is expected to provide crucial information for cancer research and clinical applications.

Materials and methods

Chemicals

Ultrapure water (Millipore Milli-Q) was used throughout the work. High glucose Dulbecco's Modified Eagle Medium (DMEM) and RPMI-1640 media were purchased from HyClone (Thermo scientific, IL, USA). Fetal bovine serum (FBS) and trypsin EDTA was purchased from Gibco BRL Co. Ltd. (USA). ICP-MS multi-element standards containing Fe, Zn, Cu, and Mn (10 μg/mL) were purchased from PerkinElmer, Inc. The single element standard solution of P and S (1000 μg/mL) were purchased from National Center of Analysis and Testing for Nonferrous Metals and Electronic materials (Beijing, China). Methanol (99.9%, ACS/HPLC Certified) was obtained from J&K Chemical Ltd (Beijing, China).

Cell culture and treatment

Three different human cell lines, including cervical cancer cell (HeLa), lung carcinoma cell (A549), and normal human bronchial epithelial cell (16HBE) were used in the study. HeLa and A549 cell lines were obtained from the American Type Culture Collection (ATCC). 16HBE cell was purchased from Cell Bank in Peking Union Medical College. HeLa cells were cultured (37 °C, 5% CO_2) in DMEM medium supplemented with 10% FBS (Gibco) and 1% Penicillin-Streptomycin Solution. A549 and 16HBE cells were cultured in complete culture medium containing RPMI-1640. The cells during the log growth phase were collected *via* digestion with trypsin EDTA, centrifuged at 1200 rpm for 3 min, and washed with 0.9% NaCl solution for 3 ~ 4 times. For single cell analysis, the collected cells were immobilized with methanol at 4 °C, centrifuged to remove methanol, and resuspended in ultrapure water with a cell number density at 10^5/mL. The number of cells was

counted by hemacytometer. For the measurement of total cells, the cells were digested with 1 mL of concentrated nitric acid (MOS grade) at 90 °C for 2 h. Then the digested solution was diluted with 2% HNO_3 and determined by ICP-MS.

Time-resolved ICP-MS measurement

The quadrupole-based PerkinElmer NexION 300D ICP-MS equipped with a concentric PFA-ST nebulizer and a baffled quartz cyclonic spray chamber was used throughout the experiment. The ICP-MS instrumental and operating parameters for SCA and bulk analysis are listed in Table 1. Before analysis, the ICP-MS was tuned using a 10 μg/L multi-element standard solution (containing Li, Be, Mg, Fe, In, Ce, Pb, U in 2% v/v nitric acid). In order to eliminate polyatomic interferences and obtain high signal-to-background ratio (SBR), $^{56}Fe^+$, $^{68}Zn^+$, $^{63}Cu^+$ and $^{55}Mn^+$ in single cells was measured separately in dynamic reaction cell (DRC) mode using NH_3 as a reaction gas. Phosphorus (P) and sulfur (S) was measured in DRC mode by using O_2 as a reaction gas, and monitored *via* the oxide reaction products PO^+ at m/z 47 and SO^+ at m/z 48 as the analytical species. The reaction gas rate, from 0.3 mL/min to 1.2 mL/min with a step of 0.1 mL/min, and the quadrupole rejection parameter q (RPq), from 0.4 to 0.8 with a step of 0.05, were optimized based on obtaining the lowest background equivalent concentrations (BEC) by using the 10 μg/mL standard solution. The dwell time (t_{dwell}) was optimized from 0.1 ~ 20 ms and the cell density for test was optimized from 5×10^4/mL to 1×10^6/mL.

Data processing

For SC-ICP-MS, an iterative algorithm based on a three times standard deviation (3σ) was used to distinguish single cell events from the background signal.[24] Briefly, the mean and standard deviation (σ) of the entire dataset are firstly calculated and the data that are 3σ above the mean were collected. The reduced dataset is recalculated with the same method until no data points are higher than 3σ the final mean. The mean value of the entire data set plus 3σ is considered as the threshold value of the cellular contents, at which equal or below this value are excluded. The collected data represent the SC signals and the reduced data represent the cellular background. The detection limit of Fe, Cu, Zn, Mn, P and S in tested cells was calculated from 3σ cellular background. The frequency of the signals was directly related to the number

of cells and the intensity of single-cell events was related to the mass of analyzed ion in one individual cell. To quantitatively analyze the mass of the elements in a single cell, the multi-element standards containing Fe, Cu, Zn, Mn, P and S were measured under the conditions of SC as well. Box plots and Gauss/Poisson statistics was used to visualize the distribution patterns of these elements in individual cells.

Results and discussion

Single cell analysis by time-resolved ICP-MS

For SC-ICP-MS analysis, the tested cells keeping intact cellular morphology and staying in monodispersed state is important, so that each ICP-MS spike signal corresponds to one individual cell event.[9] The light microscope observation showed that the cells remained morphological integrity and were well monodispersed in aqueous solution (Fig. 1).

The difficulty for SC-ICP-MS measurement is that the matrix of cells are composed primarily of light elements C, H, O, and N, which easily generate polyatomic interferences (such as the polyatomic interference of $^{40}Ar^{16}O^{+}$ and $^{40}Ca^{16}O^{+}$ on $^{56}Fe^{+}$) that regularly masks the single cell events, particularly for the masses between 40 and 82 amu. The DRC technique can help to remove these interferences by using gas-phase chemical reactions. In the present study, NH_3 was used as the highly reactive gas to react with the interference ion for analysis of ^{56}Fe, ^{63}Cu, ^{68}Zn, and ^{55}Mn. P and S were detected *via* $^{47}PO^{+}$ and $^{48}SO^{+}$ as analyte ions using O_2 as a reaction gas in DRC to oxidize S^{+} and P^{+}. Fig. 2 presents the effects of the parameters of reaction gas flow rate and RPq on the BEC measurements. The optimized parameters for the analysis of $^{56}Fe^{+}$, $^{63}Cu^{+}$, $^{68}Zn^{+}$, $^{55}Mn^{+}$, $^{47}PO^{+}$ and $^{48}SO^{+}$ are listed in Table 1. Under the optimized condition, the reaction gas flow rate of 0.7 mL/min and RPq as 0.65 resulted in the lowest BEC (0.08 μg/L) for ^{56}Fe measurement (Fig. 2).

In order to obtain sensitive and accurate signals of single cells by ICP-MS, the number density of cells must be controlled properly and only one cell should be

transported to the plasma at any given time (t_{dwell}). Fig. 3 shows the effects of cell density on signal profile. The cell events increased with the increase of cell density from 5×10^4/mL to 2×10^5/mL, while they decreased when the concentration was higher than 5×10^5/mL, which might be caused by the overlapping of cell signals. As a result, the cell density of 2×10^5/mL was chosen.

Fig. 4 presents the temporal profile of ^{56}Fe in single Hela cells (2×10^5 cells/mL) by ICP-MS at various t_{dwell}. The data show the number of single cell events per min gradually increased with the t_{dwell} from 0.1 to 5 ms, and reach a maximum at the t_{dwell} of 5 and 10 ms, and then decreased with the t_{dwell} to 20 ms (Fig. 5). Therefore, the t_{dwell} of 5 ms is proved to ensure the best SBR. It is known that the dwell time and settling time determines the transient data acquisition speed of time-resolved ICP-MS, which is important for SCA.[23,25] Generally, a minimum dwell time and no settling time is a desirable situation for SCA. It has been reported that a cell event in the plasma lasts 0.2-0.4 ms.[26] When the settling time of the data acquisition is shorter than the t_{dwell}, the longer t_{dwell} than the duration of ion plume generation will result in low spike signals that correspond to cell events, which is due to the signal average with the background in this time window. Thus, a short t_{dwell} is generally desirable to obtain high SBR. However, when the settling time of the data acquisition is longer than the $t_{dwell,}$ an inappropriate short t_{dwell} will decrease effective reading frequency and waste the detection time. In the study, when operation in DRC mode, an appreciable settling time (~ 4 ms) is required for the processes, including the charge distribution, ion flow from cell entrance to exit, and ion signal settling down to stable values. The obtained optimal t_{dwell} under cellular condition is consistent to this settling time, which can guarantee the maximum reading efficiency.

The feasibility for individual cell monitoring within the 5-ms integration window are further demonstrated by calculating the probability of two cells existence in one aerosol droplet and simultaneously entering the plasma during a t_{dwell}. The diameter of the transmitted droplets in ICP is commonly considered as 10 μm.[9] Under the conditions of 0.32 mL/min for the sample uptake rate, the rate of generating droplets aerosol is about 6.1×10^8/min, thus, for the cell number density of 2×10^5/mL, the probability of a cell presents in one aerosol droplet is calculated as about 1×10^{-4}, indicating the chance of two cells in one droplet can be ignored. In addition, the probability of two cells in ICP within the 5 ms t_{dwell} is calculated as 0.005% and the

cell transport efficiency is about 0.2% based on the average spike frequency of ^{56}Fe (approximately 2/s) and Poisson statistics,[27] indicating the spike overlapping from two cells is insignificantly under the experimental conditions.

Quantitative analysis and distribution patterns of mineral elements in single cells

The contents of Fe, Cu, Zn, Mn, P, and S in single cells were quantitatively analyzed *via* time-resolved ICP-MS and cell digestion methods, respectively. Fig. 6 shows the SC-ICP-MS temporal profiles of $^{56}Fe^+$, $^{68}Zn^+$, $^{63}Cu^+$, $^{55}Mn^+$, $^{47}PO^+$, and $^{48}SO^+$ spike signals in Hela cells, indicating the single cell events were successfully detected by the time-resolved ICP-MS. The obtained detection limits are: Fe (4 fg), Cu (0.6 fg), Zn (8 fg), Mn (0.3 fg), P (2.8 pg), S (0.8 pg), which may satisfy the requirement of SC measurement. The quantitative analysis of these elements in single cells was achieved *via* measuring the standard solutions at the same experimental conditions. Linear calibration curves for $^{56}Fe^+$, $^{68}Zn^+$, $^{63}Cu^+$, $^{55}Mn^+$, $^{47}PO^+$, and $^{48}SO^+$ (correlation coefficient $R^2 > 0.999$) were obtained and the mass of these elements in SC sample was calculated using the the following equation:

$$m_c = \frac{\eta_n \cdot Q_{sam} \cdot t_{dwell} \cdot (I_c - I_{Bgd})}{m},$$

where m_c is the mass of elements in a single cell; η_n is the transport efficiency of standard solution (about 1% in the experiment); Q_{sam} is the sample uptake rate, t_{dwell} is the dwell time of standard solution; m is the slope of the calibration curve; I_c and I_{Bgd} are the signal intensity of a single cell and the cellular background, respectively. The average masses of Fe, Cu, Zn, Mn, P, and S in Hela, A549 and 16HBE single cells determined by SC-ICP-MS are listed in Table 2, which shows good agreement with the data by the cell digestion method (Table 2), demonstrating the SC-ICP-MS is a reliable method for analysis of mineral element content in single cells.

Importantly, the data by SC-ICP-MS can provide the distribution patterns of elements in individual cells which reflect the cell variability. The relative frequency of high-intensity elemental signals in single cells follows a Gaussian distribution, whereas, at low intensity, the frequency can be described with a Poisson distribution, assuming perfectly random arrival of ions to the detector.[28] The statistical analysis shows that the distribution of ^{56}Fe, ^{68}Zn, ^{63}Cu, ^{55}Mn, ^{47}PO and ^{48}SO contents in the

three cell lines presents different patterns (Fig. 7 and Fig. 8). The spike intensity of ^{56}Fe in single Hela, A549, and 16HBE cells shows nearly log-normal distributions with a long right-hand tail, indicating a small number of cells possess high Fe contents. The full width at half maximum (FWHM) of the distribution plots of ^{56}Fe in Hela, A549, and 16HBE cells are 0.07, 0.20, and 0.17, respectively, exhibiting that the Fe contents in Hela cells are more homogeneous than in A549 and 16HBE ones. Similarly, the Zn content in single Hela, A549, and 16HBE cells shows log-normal distribution patterns as well but with a small FWHM value of 0.03, indicating the homogeneity of intracellular Zn contents in the three types of cells. The intensity distribution of Cu in single Hela cells approximately fits log-normal and has a FWHM of 0.17, whereas, in single A549 and 16HBE cells, the Cu content presents a Poisson distribution. The spike intensity of ^{55}Mn, ^{47}PO, and ^{48}SO in single-cell level of the three cells follows a Poisson distribution as well. In Poisson distribution, the parameter λ refers to the average value and the variance of distribution, which means the average intensity of events in a time interval and the width of distribution. Interestingly, the λ values of P and S distribution in Hela cells are 41 and 35, respectively, which are obviously higher than those in A549 (4 and 12, respectively) and 16HBE cells (5 and 11, respectively), indicating the single Hela cells have relatively high level and wide distribution of P and S contents comparing with A549 and 16HBE cells. Moreover, the box plots that display distribution profiles of the elemental masses in individual cells are shown in Fig. 9. It is noteworthy that the masses of Fe, Cu, Zn, Mn, P, and S in single Hela cells span a broader range of values than those in A549 and 16HBE cells, demonstrating larger biological variations in a population of Hela cells than in the other two cells. Comparatively, the masses of Cu, Zn, P, and S in 16HBE cells show the narrowest distribution among the three tested cells, indicating the homogeneity of the element contents in the single 16HBE cells.

It has been reported that tumor cells generally require larger amount of Fe, Cu, Zn, P and S than normal ones to sustain their growth and proliferation.[8,29] For instance, cancer cells (*e.g.*, Hela, breast cancer, pancreatic cancer and hepatocellular cancer) may reprogram the iron metabolism, including iron acquisition, efflux, storage and

regulation, to satisfy their iron requirement.[10] Similarly, high level of Cu is usually necessary in cancer cells, which may act as a tumor promotor to stimulate cancer-cell proliferation and regulate oxidative phosphorylation.[14] The measurement of P in single cells may be particularly useful in the identification of malignant tumor cells because cancerous cells (lung cancer, breast cancer, etc.) have a tendency to accumulate more phosphate in DNA than normal cells.[30,31] Sulfur is shown to significantly increase homocysteine levels in rapid proliferating tumor cell lines due to increase of protein synthesis and transmethylation reactions.[32] Therefore, the content discrepancies and different distribution patterns of the essential mineral elements (Fe, Zn, Cu, Mn, P, S, etc.) in single cells can be used to differentiate normal and tumor cells in a mixed population of cells.

Conclusions

Cellular heterogeneity that arises from stochastic changes of genes, proteins, metabolites and so forth is a fundamental principle of cell biology. Herein, the time-resolved ICP-MS for the determination of essential mineral elements: Fe, Cu, Zn, Mn, P and S, in single cells (SC-ICP-MS) have been developed. By using DRC mode to eliminate polyatomic interferences and optimizing the sample uptake rate, cell number density and effective dwell time for SC-ICP-MS analysis, the element mass can be sensitively detected and quantified at the single cell level.

The quantitative analysis by SC-ICP-MS shows obviously cellular variation of the mineral elements in Hela, A549, and 16HBE cells among individual cells. The mass of Fe, Cu, Zn, Mn, P and S in single Hela cells is significantly higher than in A549 and 16HBE cells, and they span an obviously broader range of values in Hela than in the other two types of cells, demonstrating greatly biological variations in Hela cell populations. Furthermore, the masses of Fe, Cu, Zn, Mn, P and S in the three types of cells follow different distribution patterns. In single Hela cells, Fe, Zn and Cu masses follow log-normal distributions, and Mn, P and S masses follow Poisson distributions with high λ values, indicating the large variation of the masses of elements among single Hela cells. The study demonstrates the method of SC-ICP-MS provides potential application for monitoring the variation of distribution patterns of mineral elements at the single cell level.

Acknowledgements

The authors are grateful to the support of the National Basic Research Program (973 program, 2011CB933403) and the National Natural Science Foundation of China (11275214, 21175136, 11375211).

References

1. P. K. Chattopadhyay, T. M. Gierahn, M. Roederer and J. C. Love, *Nat. Immunol.*, 2014, **15**, 128-135.
2. M. J. Gerdes, C. J. Sevinsky, A. Sood, S. Adak, M. O. Bello, A. Bordwell, A. Can, A. Corwin, S. Dinn, R. J. Filkins, D. Hollman, V. Kamath, S. Kaanumalle, K. Kenny, M. Larsen, M. Lazare, Q. Li, C. Lowes, C. C. McCulloch, E. McDonough, M. C. Montalto, Z. Pang, J. Rittscher, A. Santamaria-Pang, B. D. Sarachan, M. L. Seel, A. Seppo, K. Shaikh, Y. Sui, J. Zhang and F. Ginty, *Proc. Natl. Acad. Sci. U. S. A.*, 2013, **110**, 11982-11987.
3. K. Kleparnik and F. Foret, *Anal. Chim. Acta.*, 2013, **800**, 12-21.
4. Z. G. Xue, K. Huang, C. C. Cai, L. B. Cai, C. Y. Jiang, Y. Feng, Z. S. Liu, Q. Zeng, L. M. Cheng, Y. E. Sun, J. Y. Liu, S. Horvath and G. P. Fan, *Nature*, 2013, **500**, 593-597.
5. M. R. Speicher, *Genome Med.*, 2013, **5,** 73.
6. P. J. Aggett, *Endocrin Metab. Clin.*, 1985, **14**, 513-543.
7. M. Speich, A. Pineau and F. Ballereau, *Clin. Chim. Acta.*, 2001, **312**, 1-11.
8. J. J. Elser, M. M. Kyle, M. S. Smith and J. D. Nagy, *Plos One*, 2007, **2**. 1028
9. K. S. Ho and W. T. Chan, *J. Anal. At. Spectrom.*, 2010, **25**, 1114-1122.
10. S. V. Torti and F. M. Torti, *Nat. Rev. Cancer*, 2013, **13**, 342-355.
11. S. V. Torti and F. M. Torti, *Cancer Res.*, 2011, **71**, 1511-1514.
12. Z. K. Pinnix, L. D. Miller, W. Wang, R. D. Agostino, T. Kute, M. C. Willingham, H. Hatcher, L. Tesfay, G. Sui and X. Di, *Sci. transl. med.*, 2010, **2**, 43ra56-43ra56.
13. D. R. Richardson, *Curr. Med. Chem.*, 2005, **12**, 2711-2729.
14. S. Ishida, P. Andreux, C. Poitry-Yamate, J. Auwerx and D. Hanahan, *Proc. Natl. Acad. Sci. U. S. A.*, 2013, **110**, 19507-19512.
15. A. Gupte and R. J. Mumper, *Cancer Treat. Rev.*, 2009, **35**, 32-46.
16. S. I. Miyashita, A. S. Groombridge, S. I. Fujii, A. Takatsu, K. Chiba and K. Inagaki, *Anal. Sci.*, 2014, **30**, 219-224.
17. S. C. Bendall, E. F. Simonds, P. Qiu, A. D. Amir, P. O. Krutzik, R. Finck, R. V. Bruggner, R. Melamed, A. Trejo, O. I. Ornatsky, R. S. Balderas, S. K. Plevritis, K. Sachs, D. Pe'er, S. D. Tanner and G. P. Nolan, *Science*, 2011, **332**, 687-696.
18. L. N. Zheng, M. Wang, B. Wang, H. Q. Chen, H. Ouyang, Y. L. Zhao, Z. F. Chai and W. Y. Feng,

Talanta, 2013, **116**, 782-787.

19. T. Nomizu, S. Kaneco, T. Tanaka, D. Ito, H. Kawaguchi and B. T. Vallee, *Anal. Chem.*, 1994, **66**, 3000-3004.
20. F. M. Li, D. W. Armstrong and R. S. Houk, *Anal. Chem.*, 2005, **77**, 1407-1413.
21. C. N. Tsang, K. S. Ho, H. Sun and W. T. Chan, *J. Am. Chem. Soc.*, 2011, **133**, 7355-7357.
22. A. S. Groombridge, S. Miyashita, S. Fujii, K. Nagasawa, T. Okahashi, M. Ohata, T. Umemura, A. Takatsu, K. Inagaki and K. Chiba, *Anal. Sci.*, 2013, **29**, 597-603.
23. S. Miyashita, A. S. Groombridge, S. Fujii, A. Minoda, A. Takatsu, A. Hioki, K. Chiba and K. Inagaki, *J. Anal. At. Spectrom.*, 2014, **29**, 1598-1606.
24. H. E. Pace, N. J. Rogers, C. Jarolimek, V. A. Coleman, C. P. Higgins and J. F. Ranville, *Anal. Chem.*, 2012, **84**, 4633-4633.
25. A. Hineman and C. Stephan, *J. Anal. At. Spectrom.*, 2014, **29**, 1252-1257.
26. S. D. Tanner, D. R. Bandura, O. Ornatsky, V. I. Baranov, M. Nitz and M. A. Winnik, *Pure Appl. Chem*, 2008, **80**, 2627-2641.
27. J. W. Olesik and P. J. Gray, *J. Anal. At. Spectrom.*, 2012, **27**, 1143-1155.
28. G. Cornelis and M. Hassellöv, *J. Anal. At. Spectrom.,* 2014, **29**, 134-144.
29. M. P. Silva, A. Tomal, C. A. Perez, A. Ribeiro-Silva and M. E. Poletti, *X-Ray Spectrom.*, 2009, **38**, 103-111.
30. K. Dash, L. Rastogi and J. Arunachalam, *Analyst*, 2012, **137**, 668-674.
31. W. Wulaningsih, K. Michaelsson, H. Garmo, N. Hammar, I. Jungner, G. Walldius, L. Holmberg and M. Van Hemelrijck, *Bmc Cancer*, 2013, **13**, 257.
32. Y. Ozkan, S. Yardim-Akaydin, H. Firat, E. Caliskan-Can, S. Ardic and B. Simsek, *Anticancer Res.*, 2007, **27**, 1185-1189.

Table 1 NexION 300D ICP-MS instrumental and data acquisition parameters for cell analysis

Instrumental Parameters	SCA	Cell digestion
ICP parameters		
Nebulizer	Concentric PFA-ST	
Spray Chamber	Baffled Quartz Cyclonic	
Torch	Glass Torch	
ICP RF Power	1600 W	
Plasma Gas	18 L/min	
Auxiliary Gas	0.9 L/min	
Nebulizer Gas	1.0 L/min	0.92 L/min
Measurement parameters		
Acquisition mode	Peak Hopping	
Sweeps	1	20
Dwell time	5ms	50ms
DRC parameters		
RPa	0	
RPq	0.40 (for $^{56}Fe^{+}$), 0.45 for ($^{63}Cu^{+}$), 0.55 (for $^{68}Zn^{+}$, $^{55}Mn^{+}$, $^{47}PO^{+}$ and $^{48}SO^{+}$)	
DRC gas (NH_3)	0.7 mL/min (for $^{56}Fe^{+}$ and $^{55}Mn^{+}$), 0.5 mL/min (for $^{68}Zn^{+}$), 0.9 mL/min (for $^{63}Cu^{+}$)	
DRC gas (O_2)	2.2 mL/ min (for $^{47}PO^{+}$ and $^{48}SO^{+}$)	

Table 2 Quantitative analysis of elements in single cells by SC-ICP-MS and cellular digestion ICP-MS

Elements	Analytes	Hela		A549		16HBE	
		SC	Digestion	SC	Digestion	SC	Digestion
Fe (fg)	$^{56}Fe^{+}$	26.6±2.6	22.3±2.7	17.2±1.6	16.2±1.3	15.1±1.0	11.3±1.0
Zn (fg)	$^{68}Zn^{+}$	72.9±5.7	68.4±4.0	42.9±4.9	31.5±2.4	25.7±1.4	27.4±0.7
Cu (fg)	$^{63}Cu^{+}$	3.7±0.8	3.4±0.3	1.6±0.2	1.4±0.1	1.4±0.1	2.1±0.1
Mn (fg)	$^{55}Mn^{+}$	0.5±0.1	0.6±0.1	0.4±0.0	0.4±0.0	0.2±0.0	0.2±0.0
P (pg)	$^{47}PO^{+}$	8.9±0.1	14.6±1.3	4.7±0.1	6.7±0.5	5.2±0.5	5.1±0.4
S (pg)	$^{48}SO^{+}$	6.1±0.1	5.2±0.5	2.7±0.1	3.7±0.3	1.3±0.1	1.8±0.1

Figure captions

Fig. 1 Microscope images of Hela (a), A549 (b) and 16HBE (c) cells in ultrapure water after immobilization with 70% v/v methanol.

Fig. 2 BEC concentration histogram with the reaction gas flow rate and RPq.

Fig.3 Effects of cell density on signal profile of single cells.

Fig. 4 ICP-MS temporal profile of ^{56}Fe in Hela cells with a cell number density of 2×10^5 cells/mL at different t_{dwell} ranging from 0.1 to 20 ms.

Fig. 5 Single cell event rate at different t_{dwell}.

Fig. 6 ICP-MS signal profile of $^{56}Fe^+$, $^{68}Zn^+$, $^{63}Cu^+$, ^{55}Mn, and $^{47}PO^+$ and $^{48}SO^+$in Hela cells at a cell number density of 2×10^5 cells/mL.

Fig. 7 Intensity distribution patterns of Fe, Zn, Cu, and Mn in Hela, A549 and 16HBE cells.

Fig. 8 Intensity distribution patterns of P and S in Hela, A549 and 16HBE cells.

Fig. 9 Box plot for the mass of Fe, Zn, Cu, Mn, P and S in Hela, A549 and 16HBE cells. The boxes mark the intervals between the 25th and 75th percentiles; the lines inside the boxes denote medians; whiskers denote the intervals between the 5th and 95th percentiles and filled circles indicate data points outside the 5th and 95th percentiles.

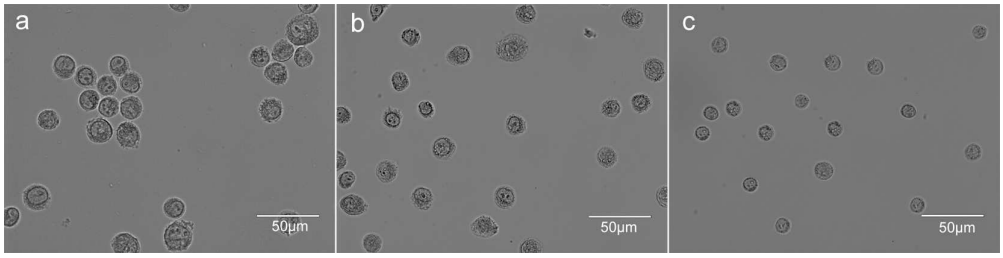

Fig. 1

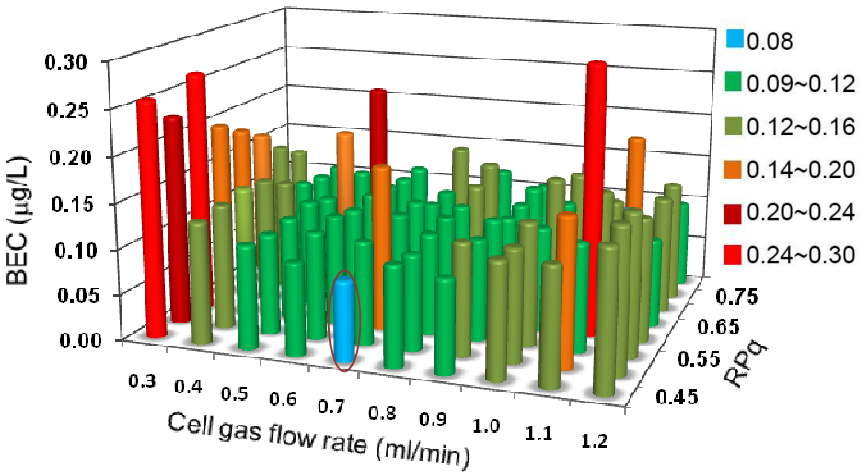

Fig. 2

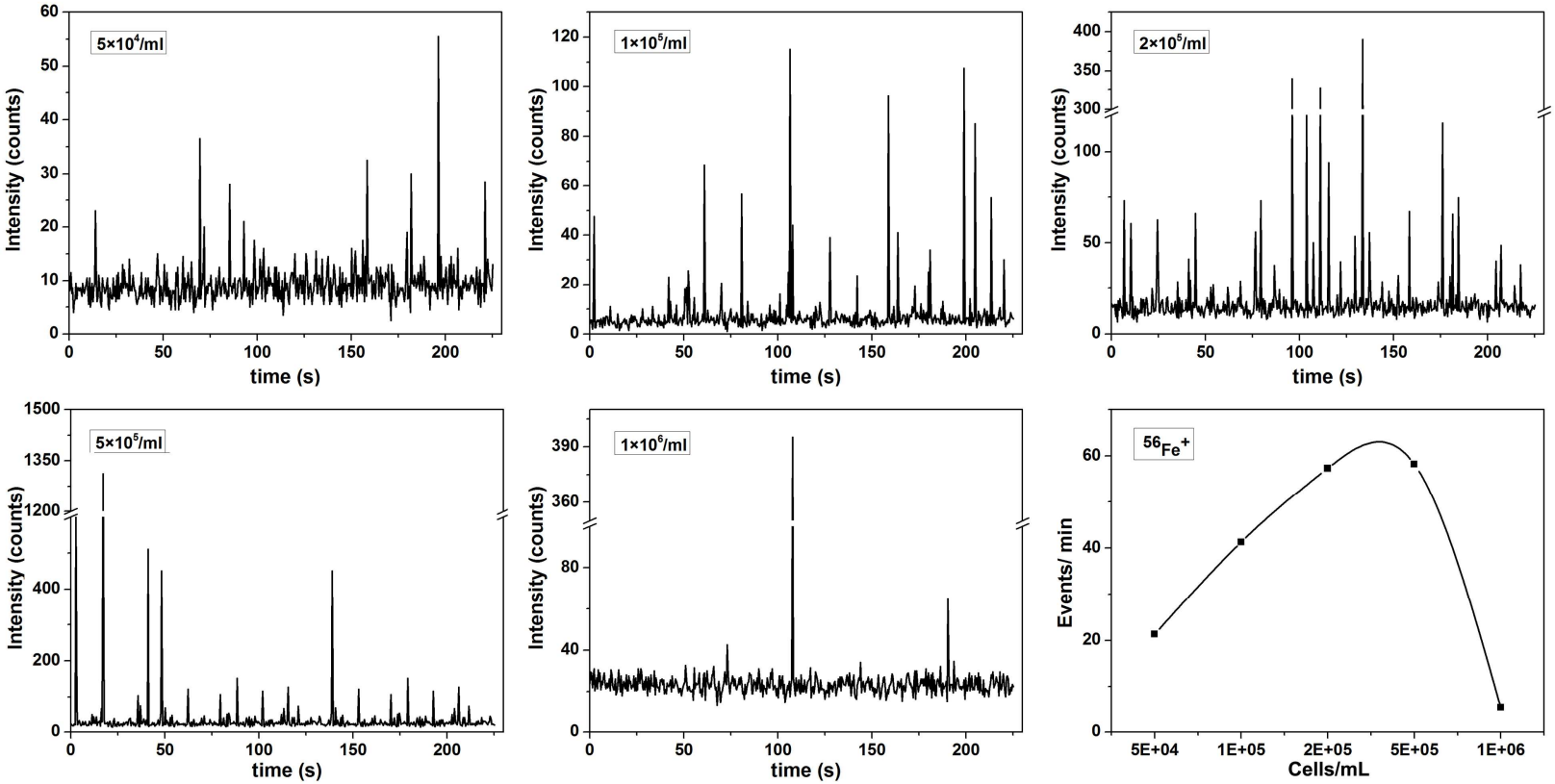

Fig.3

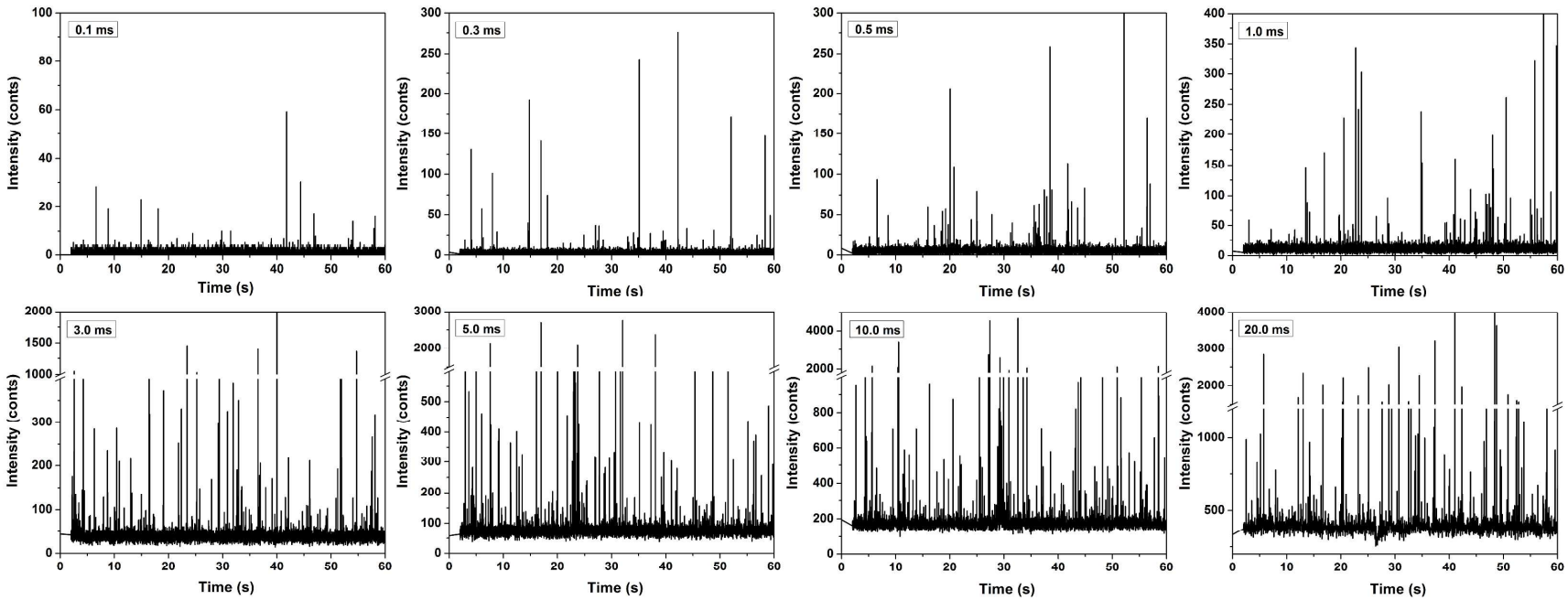

Fig. 4

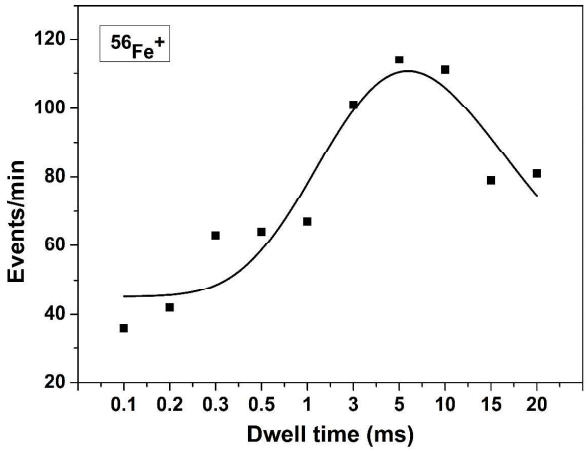

Fig. 5

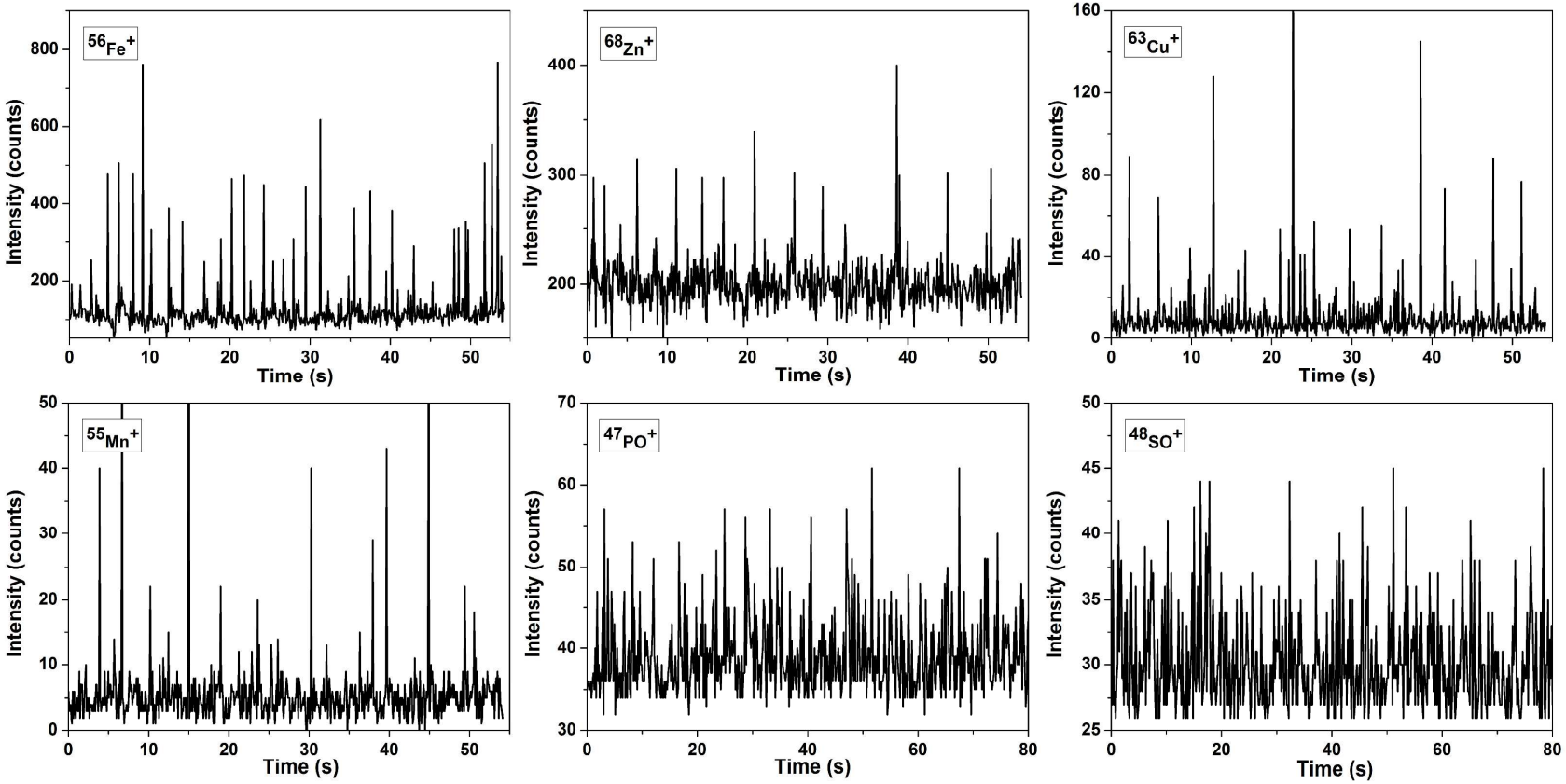

Fig. 6

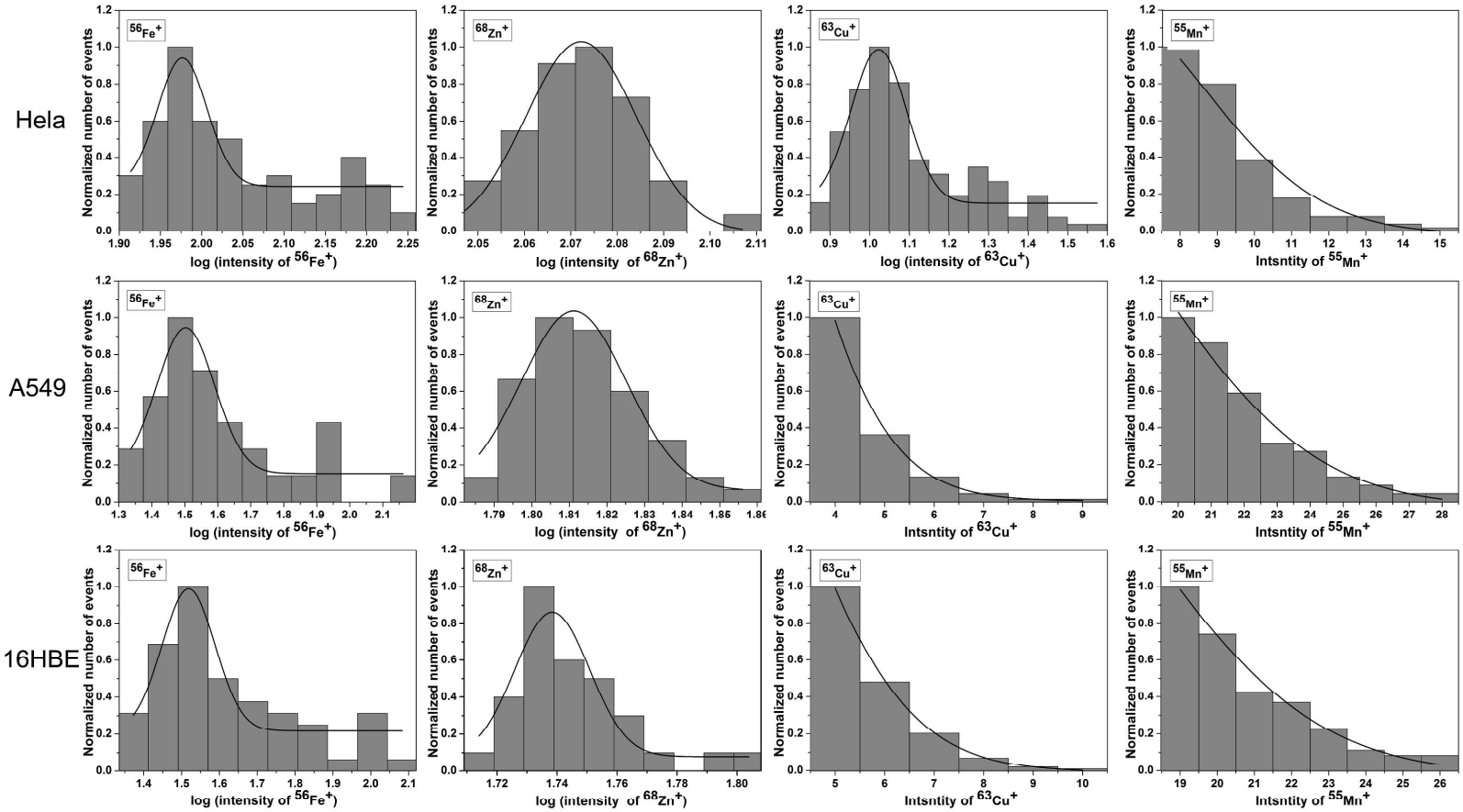

Fig. 7

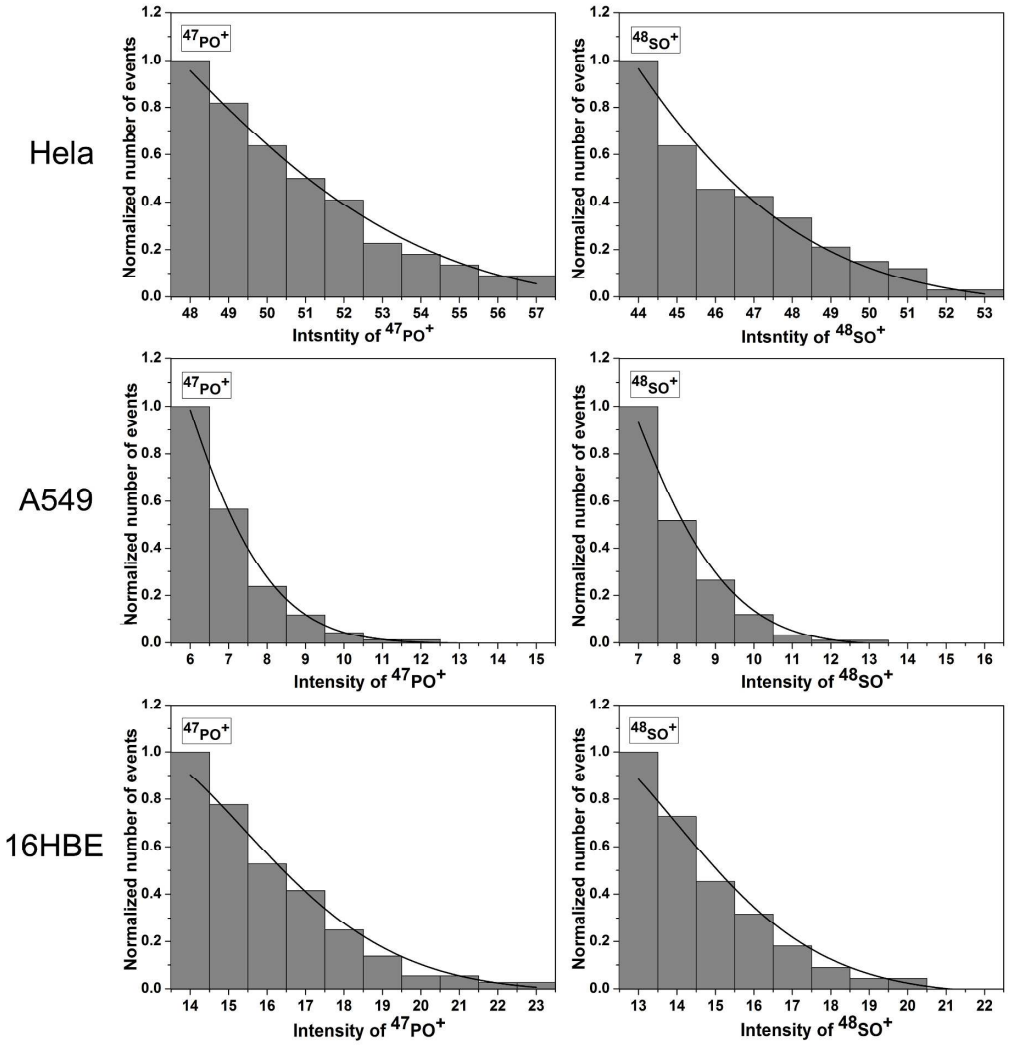

Fig. 8

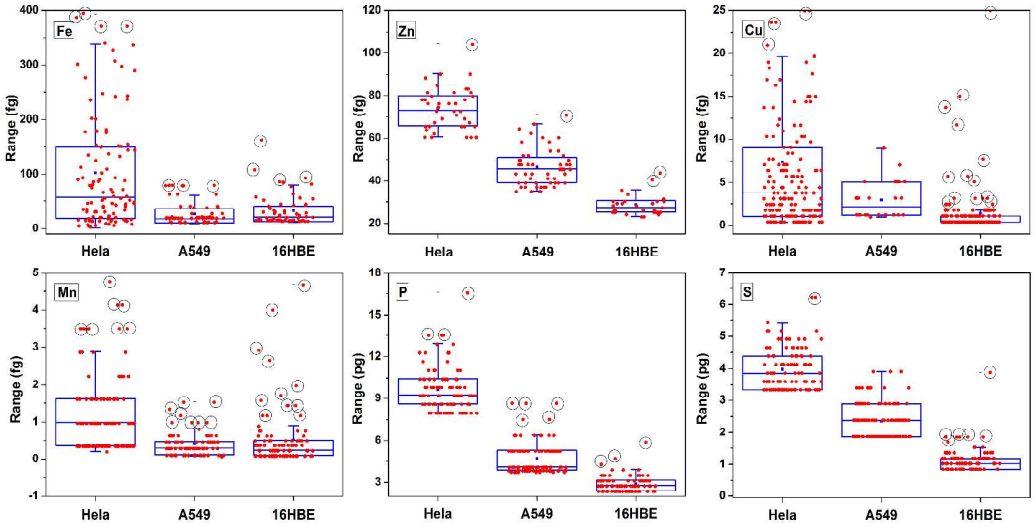

Fig.9